Fire-resistant bio-based polyurethane foams designed with two by-products derived from sugarcane fermentation process

Ana Paula Capêto
Universidade Católica Portuguesa Escola Superior de Biotecnologia: Universidade Catolica Portuguesa Escola Superior de Biotecnologia

Manuela Amorim
Universidade Católica Portuguesa Escola Superior de Biotecnologia: Universidade Catolica Portuguesa Escola Superior de Biotecnologia

Sérgio Sousa
Universidade Católica Portuguesa Escola Superior de Biotecnologia: Universidade Catolica Portuguesa Escola Superior de Biotecnologia

Joana R. Costa
Universidade Católica Portuguesa Escola Superior de Biotecnologia: Universidade Catolica Portuguesa Escola Superior de Biotecnologia

Braian Uribe
Universidade Católica Portuguesa Escola Superior de Ciências e Tecnologia: Universidade Catolica Portuguesa

Ana Sofia Guimarães
Universidade do Porto Instituto de Materiais Núcleo FEUP: Universidade do Porto Faculdade de Engenharia

Manuela Pintado
Universidade Católica Portuguesa Escola Superior de Biotecnologia: Universidade Catolica Portuguesa Escola Superior de Biotecnologia

Ana L. S. Oliveira (asoliveira@ucp.pt)
Universidade Católica Portuguesa Escola Superior de Biotecnologia: Universidade Catolica Portuguesa Escola Superior de Biotecnologia https://orcid.org/0000-0001-5445-1032

Research Article

Keywords: Sugarcane bagasse ash, microbial oil, polyurethane foam, fire-resistant, bio-based

Posted Date: May 2nd, 2023

DOI: https://doi.org/10.21203/rs.3.rs-2704397/v1

Version of Record: A version of this preprint was published at Waste and Biomass Valorization on September 15th, 2023. See the published version at https://doi.org/10.1007/s12649-023-02274-6.

Abstract

There is a great interest in replacing conventional fossil-based polymers and composites with inorganic or organic waste-based materials and filler-type additives, to promote environmental sustainability and circularity. The main objective of this study was the design of water-blown polyurethane rigid foams integrating two by-products derived from the Amyris fermentation process of production of β-farnesene. The distillation residue (FDR) was used as main polyol component in the neat formulation of the foams (PF) that it was supplemented (PFA) with 4.5% of sugarcane bagasse ash (SCBA) added as a filler with fire-retardant properties. The impact of both by-products on the foam density and morphology, and in the thermal, mechanical, and flame-retardant properties was assessed. SCBA presence led to a reduction in apparent density, cells size, and glass transition, delaying the thermal decomposition. The differences observed in the thermal conductivity and flammability test parameters suggest a visible impact of the ash incorporation, thus meeting the fire protection standard UL 94, class HB.

Highlighting the need for further optimization, this work presents a practical example of the integration of different wastes derived from the same fermentation process in the formulation of sustainable PUR foams with reduced flammability.

1. Introduction

The circular economy is already recognized as a regenerative system model that endorses the efficient use of resources through waste minimization, long-term value retention, reduction of primary resources, and closed loops of materials within the boundaries of environmental protection and socio-economic benefits [1].

The increasing awareness of petroleum reserves depletion [2, 3], together with subsequent floating prices triggered the implementation of sustainable technologies to reduce the environmental impact and minimize the footprint of fossil-based plastics replacing them with bio-based materials [4].

Polyurethane foams are usually the product of a polymerization reaction between an isocyanate (e.g., methyl diphenyl diisocyanate, MDI) and a fossil-based polyol, blended using customized formulations that depends on the final application and generally involve the use of catalysts, surfactants, blowing agents, chain extenders, etc. [5, 6]. That reaction results in a cellular structure characterized by resistance to water exposition, relevant mechanical properties, and low thermal conductivity coefficients, ensuing their application, for example, in furniture, bedding, and thermal-insulating systems, such as refrigerating units, pipe and roof insulation and wall padding for building purposes [7–9].

In the last decades, the need to replace non-renewable feedstock led to the synthesis of bio-based polyols using a range of natural renewable resources has been the subject of expanded research [10, 11]. The feedstock ranges from edible oils (e.g. soybean, sesame, and sunflower oils), to biomass lignocellulosic residues and non-edible vegetable oils which don´t compete with the food industry, such as castor,

jatropha, and neem oils, etc. [12]. Other oily wastes are also subject of many studies, for example, waste cooking oil [13], fish oil [14], and microbial oils [15, 16].

The chemical composition, low density and air permeability of polyurethane foams promotes flammability, enhancing fire expansion [17]. To counteract this effect, and to reduce combustibility and suppress toxic fumes or smoke production, have been used flame retardants, e.g. inorganic fillers, organic phosphorous compounds, nitrogen-based materials, and halogenated materials [17, 18]. Biomass ash derived from industrial by-products such as rice husk or sugarcane bagasse, is a natural and suitable eco-friendly waste material with a high content in silica, which is known to act as flame retardant, improving thermal stability and mechanical properties in polyurethane foams [19–21]. Recently a research study revealed that the incorporation of 50% of waste ash improved heat release by 69% and reduced CO_2 and CO emissions by 76 and 77%, respectively, during a fire [22].

Amyris patented brand molecule called trans-ß-farnesene is synthesized using conventional fermentation of sugar syrup from sugarcane by genetically modified Saccharomyces cerevisiae [23, 24]. This process generates a distillation residue, a microbial oil composed by a certain amount of wax esters (0.22% wt.), hydrocarbons (43.29%), a small percentage of complex lipids such as tri- and di-glycerides along with farnesol, terpenes such as β-farnesene, sesquiterpenes, and triterpenes [25]. The chemical profile akin to vegetable oils and the iodine value around 122 gI_2/100g indicates a certain degree of unsaturation and the possibility to synthesize polyols for condensation polymers, exemplified by the polyurethane class, which implies a set of chemical reactions to achieve the necessary functionalization that explores carbon-carbon double bonds and ester linkages present in natural oils [26–28].

The main purpose of this manuscript was to use this microbial oil residue to produce a polyol that will represent the polyurethane backbone in a formulation supplemented with sugarcane bagasse ash, as a flame-retardant additive. The properties of the formulated bio-based polyurethane foams will be discussed.

2. Materials and Methods

Materials and Reagents

β-farnesene distillation residue (FDR), (iodine number of 122 g I_2/100 g) was provided by Amyris Inc. (Campinas, Brazil) and characterized elsewhere [25]. Sugarcane bagasse ash (SCBA) with % of organic matter, was provided by Raizen /Amyris (Brazil). Both materials were transported from Brazil to the CBQF-UCP laboratory (Porto, Portugal) under refrigerated conditions. Glycerol (9 %) and ethyl acetate were supplied by Carlo Erba and formic acid (9 %) by Honeywell Fluka. Ethanol (9 %), hydrogen peroxide (3 %) and sodium hydrogen carbonate by Labchem. Sigma–Aldrich supplied analytical grade reagents such as hydrofluoric acid (HF 4 %), nitric acid (HNO_3 6 %), phosphoric acid (85%), potassium hydroxide standard solution, pyridine (99%), acetic anhydride, 1-butanol, phenolphthalein indicator, dibutyltin dilaurate

(DBTDL), poly (dimethyl siloxane) (PDMS), 4,4- diphenylmethane diisocyanate (4,4-MDI) and HPLC grade tetrahydrofuran.

Procedure

Pretreatment of the filler Sugarcane bagasse ash (SCBA) was subjected to a thermochemical pretreatment to oxidize the organic matter present in the received samples. The ash was loaded in a porcelain crucible placed in a laboratory muffle and heated from room temperature to 600°C at a rate of 10°C min^{-1}, followed by a stage at 600°C for 5 h. After cooling to room temperature, 1 mL of hydrogen peroxide was with 15 g of ash, was, and the sample proceeded to another 600°C cycle. The treated ash, presented an apparent density of 1400 $kg.m^{-3}$, and particle size lower than 250 µm.

Polyol synthesis was carried out by a simple two-step mechanism of FDR epoxidation with performic acid formed *in situ* according to the method described elsewhere [15, 29], followed by oxirane ring-opening with phosphoric acid. FDR (200 g), ethyl acetate (100 g), and formic acid (12 g) were weighed in a closed borosilicate vessel with a three-way lid and placed on a heating/stirring plate (Hei-Tech, Heidolph Instruments GmbH & Co.KG, Schwabach, Germany). After a few minutes of constant stirring, refrigerated hydrogen peroxide (320 g) was slowly poured to avoid exothermic foaming. The epoxidation took place at 65°C for 6 h with constant stirring, followed by decantation of the organic phase in a separatory funnel and a neutralization/washing operation with water and sodium bicarbonate solution (10%). The epoxide was then dried overnight at 80°C in a vacuum oven (Binder, model VD23).

In the next step, the epoxide and phosphoric acid, ratio 7:1 wt. were loaded in the reactor vessel and heated until 85 °C for 1h. The neutralization/purification operation was conducted in the same way.

This technique is commonly used to insert hydroxyl groups in the structure exploring carbon-carbon double bonds and ester linkages present in natural oils [30]. The reaction yield (wt%) was determined by Eq. (1).

$$\text{Yield}\ (\%) = \frac{m_{\text{polyol}}\ (g)}{m_{\text{FDR}}\ (g)} \times 100 \qquad \text{Eq. (1)}$$

Polyurethane foams preparation Two formulations (Table 1) were developed for both bio-based polyurethane foams with ash (PFA) and without ash (PF). Water was used as a green reagent to react during the polymer network formation by in situ generation of the blowing agent carbon dioxide (CO_2) [31]. In the first stage all ingredients, with exception of 4,4-MDI, were weighed into a beaker and melted, in a hotplate while mechanically mixed for 2 minutes. In the second stage, the pre-measured MDI was added, and the content was manually stirred for 8–20 s. The free-rising foam was left to cure and stabilize for 48 h at room temperature [32].

Table 1
The formulation used for FDR-based water-blown PUR foam synthesis, basic foam (PF) and ash-reinforced (PFA).

Sample	Role	Amount (%)	
		PF	PFA
FDR-based Polyol	Monomer	17.7	16.9
Water	Blowing agent	1.2	1.2
Glycerol	Chain-extender	19.0	18.1
DBTDL	Catalyst	0.8	0.8
PDMS	Emulsifier	2.8	2.7
4,4'-MDI	Monomer	58.5	55.8
SCBA	Fire-retardant		4.5

Materials Characterization

Sugarcane bagasse ash (SCBA)

Quantification of minerals in SCBA was performed by Inductively Coupled Plasma – Atomic Emission Spectrometry (ICP-AES). Briefly, 250 mg of the oxidized ash was mixed in a Teflon vessel with 2 mL of HNO_3 and 2 mL of HF and heated in a microwave system (Berghof, Eningen, Germany). The digestion procedure was conducted in four steps: 140 ˚C and 40 bar for 5 min; 160 ˚C and 40 bar for 10 min; 200 ˚C and 40 bar for 30 min; 100 ˚C and 20 bar for 5 min. After microwave digestion, the samples were cooled down to room temperature and diluted to a final volume of 50 mL. Microwave-digested samples were then analyzed through ICP-AES (PerkinElmer, Massachusetts, USA) and quantified through external standard calibration. All the analyses were performed in triplicate.
FDR-based Polyol characterization

Acid number and hydroxyl (-OH) value were determined by titrimetric analysis following ASTM D4662-08 and ASTM 1957-86, respectively.

Viscosity was measured at 25.0 ± 0.1 °C, following the standard ASTM D4878-15 using a rotational viscometer from Rheology Instruments, model Lamy B-One Plus.

Molecular weight distribution was determined by high-performance liquid chromatography (HPLC). The chromatograms were acquired using an HPLC (model 1260 Infinity II, Agilent Technologies, Santa Clara, CA, USA) attached to an Evaporative Light Scattering Detector (ELSD, 1290 Infinity II, Agilent Technologies, Santa Clara, CA, USA) with evaporation temperature at 70°C and nebulization at 65°C, using nitrogen as nebulizing gas coupled to a TSK gel GMHxL column for insoluble polymers. The

isocratic analysis was carried out with tetrahydrofuran as the mobile phase; flow rate of 0.6 mL min^{-1}; sample concentrations of 20–25 mg mL^{-1} dissolved in THF and injection volumes of 20 µL. The molecular weight was estimated by calibration curve of polystyrene standards 400–303.000 Da (Agilent (Waldbronn, Germany).

Polyol functionality (f) was calculated based on the average molecular weight (M_w) and equivalent weight (E) based on the -OH value, defined by Eq. (2).

$$f = \frac{\mathrm{M_w}}{\mathrm{E}} \text{ where } \mathrm{E} = \frac{1000 \times 56.1}{[-\mathrm{OH}]} \text{ Eq. (2)}$$

Fourier Transform Infrared Spectroscopy (FTIR) was used to envision the chemical structure of all materials in the near-infrared range. Analyses were conducted in the absorbance range of 4000 to 500 cm-1, using a Perkin Elmer FT-IR spectrophotometer, fitted with a Pike Miracle ATR accessory containing Zn/Se crystal.

Polyurethane foams

Apparent density was determined as the ratio of sample weight to its volume following ASTM D1622/D1622M-14. The results represent the mean values calculated from six independent measurements.

Compressive strength was determined following the ASTM D1621-00 guidelines. The test samples were cut into cubes, and the experiment was carried out using a heavy-duty platform (HDP/90) with a 5 mm stainless steel cylindrical probe (P/0.5R) with a 30 kg load cell attached to a TA.XT 2i Texture Analyzer (Stable Micro Systems, Godalming, U.K.). The compression force was applied in the foam rise direction, with a pre-test speed was set at 1 mm. s^{-1}, the test speed was 1.70 mm. s^{-1}, and the post-test speed was 10 mm. s^{-1}. Three measurements for each replica were performed at each experimental condition tested. The compressive strength was calculated as the value of the maximum force divided by the initial cross-sectional area of each sample when the maximum applied force occurred approximately at 10% of deflection. The specific compressive strength is the ratio between the compressive strength and the apparent density and is expressed in $m^2.s^{-2}$.

Thermal properties were determined by differential scanning calorimetry (DSC) analyses were carried out using a NETZSCH DSC204 calorimeter. Nitrogen was used as the purge gas at 40 mL. min^{-1}. Approximately 2 mg of each sample was placed in aluminum pans and the thermal properties were recorded between − 50 and 200°C at 10°C·min^{-1} to observe the glass transition temperature. The glass transition temperatures (T_g) were measured on the second heating ramp to erase the thermal history of the polymer.

Thermal conductivity was determined following EN 10456 guidelines using a thermal analyzer (Isomet 2114, Applied Precision) with a surface probe (IPS 1105) and a calibration standard (XPS, IBER Fibran).

The samples dimensions were 100 mm × 100 mm × 40 mm, and the results, expressed in $W.m^{-1}.K^{-1}$ are the mean values calculated from three independent measurements.

Morphology analysis was performed by Scanning Electron Microscopy (SEM) using a JSM-5600LV (JEOL; Tokyo, Japan). Samples with 3 mm × 5 mm sliced with a scalpel from the center of the foam were placed directly on top of double-sided adhesive carbon tape (NEM tape, Nisshin, Japan), covering metallic stubs, and coated with gold/palladium using a sputter coater (Polaron, Bad Schwalbach Germany). All observations were performed using the secondary electron (SE) detector, with the SEM operated in high-vacuum, at an acceleration voltage of 15 kV and a spot size of 20. The average pore diameters were determined using ImageJ 1.53e software (USA).

Flammability test of rigid polyurethane was performed following the ASTM UL 94 HB standard for safety. This standard describes a set of a small-scale reaction test methods covering the flammability of new polymeric materials used for parts in devices and appliances and they are intended to serve as a preliminary indication of their acceptability with respect to flammability for a particular application. In this test a standard test specimen of 50 (W) · 150 (L) · 13 (H) mm of both polyurethane foams was exposed to a horizontal flame for 10 s, forcing its ignition. After that period of time the flame was extinguished, and the samples free burning characteristics were observed.

3. Results and Discussion

SCBA characterization

In the polymer industry, natural alternatives of silica have been used as inorganic fillers obtained from recycling residues to reinforce polymers composites [33]. The mineral composition of the sugarcane bagasse ash used in this study is detailed in Table 2. As expected, silica was the major mineral component, reaching almost 60 wt.%. Although the composition is dependent on several factors such as region or local temperature range, sugarcane bagasse is described to have a silica composition ranging from 55 to 90%, and some authors described sugarcane ash with a similar silica concentration (Rovani et al., 2018; Souza et al., 2011; Jiménez-Quero et al., 2013; Khalil et al., 2021). Iron oxide was the second most abundant compound in sugarcane ash, corresponding to 17.8 wt %. Although this value is unusually high for this type of biomass, some authors described similar concentrations of iron oxide in sugarcane bagasse, ranging from about 15 to 29 wt.% (Patel et al., 2018; Kawade et al., 2013).

Table 2
Sugarcane bagasse ash (SCBA) mineral composition.

Compound	Concentration (g/100 g)
SiO_2	59.5 ± 3.1
Fe_2O_3	17.8 ± 0.0
K_2O	2.5 ± 0.0
CaO	2.2 ± 0.2
P_2O_5	1.3 ± 0.1
Al_2O_3	0.9 ± 0.1
MgO	0.9 ± 0.0
Na	0.2 ± 0.0
MnO_2	0.1 ± 0.0

Polyol characterization

Polyol reactivity depends upon characteristic properties such as chemical structure, hydroxyl (-OH) value, and acid number and functionality.

The characteristics of the FDR-based polyol are described in Table 3. The reaction yield for polyol production based on the initial FDR mass, was high (around 80%) which is an important factor attending economic viability. The polyol showed a relatively low molecular weight (around 2711 Da), paired with a relatively high functionality (around 4), a low -OH value (82.3 mg KOH/ g polyol), and a high viscosity at room temperature (13256 mPa.s).

Table 3
Polyol characterization.

Measured property	Units	FDR-based Polyol
Acid value	mg $KOH.g^{-1}$	3.3 ± 1.0
Hydroxyl (-OH) value	mg $KOH.g^{-1}$	82.3 ± 0.9
Viscosity at 25 °C	mPa.s	13256
Molecular weight	Da	2711.3 ± 10.0
Functionality (f)	-	4.0 ± 0.1
Yield	%	80.3 ± 11.4

The polyol functionality gives information about chemically active atoms or groups per molecule and high values of functionalities (3–5) are expected to produce rigid foams since they have greater chances of being incorporated into the network due to a great number of reactive sites [34, 35]. The formation of hydroxyl groups with the ability to form intramolecular H-bonding or the higher content of oligomers may contribute to the high viscosity observed on the polyol [36]. The hydroxyl value may be very variable, when are compared values reported for polyols synthesized from vegetable oils. Examples of that, are the canola and palm oils with higher -OH values of 267, 222 mg KOH/g of sample, respectively [15], while others obtained from soybean, linseed, and palm oil, exhibited lower values around 90 and 78 mg KOH/g [37, 38]. Those differences may be attributed to different ring-opening agents and reaction conditions used in those studies.

The incorporation of natural oils in polyol synthesis is generally associated with some difficulties in the formulation of polyurethane foams due to their functionality, high viscosity, and low hydroxyl numbers that may affect foam properties like stability, strength, and glass transition. [39, 40]. However, the material has a versatile composition, is biodegradable, non-toxic, and environmentally friendly [41].

Structural analysis (FTIR) of all materials

The progression of the polyol and polyurethane synthesis is on Fig. 1a. The FDR lipidic content was characterized by the presence of a band at 1744 cm^{-1} assigned for C = O stretches of the ester functional groups from lipid triglycerides and fatty acids, CH_2 bands of unsaturated fatty acids that were exhibited in the range 2868 to 2969 cm^{-1} [42, 43].

In the first reaction stage, the epoxide structure presented carbonyl –C = O stretching vibrations at 1729 cm^{-1} and the enhancement of the bands characteristic of epoxy groups/oxirane rings at 866 and 833 cm^{-1}, that were already present in the condensed residue. In the second stage, when the polyol was produced, those bands decreased in intensity and emerged the typical band of –OH stretching (Fig. 1a) at about 3462 cm^{-1}. The presence of such bands confirmed the attachment of the hydroxyl groups [15].

The developed bio-based formulations (PF and PFA in Table 1) resulted in rigid polyurethane (PUR) foams and the comparative structural analysis is in Fig. 1b. Looking specifically into PF and PFA results, it was found that the polyol related -OH stretching band at 3462 cm^{-1} disappears (Fig. 1b) and new bands emerged following the reaction between -OH, -NCO (from 4,4- MDI) and additives. For instance, at 3309 cm^{-1} it was detected a band assigned to -NH stretching, as well C = O stretching (amide I) band at 1702 cm^{-1}, the amide II band at 1507–1540 cm^{-1} and the amide III band at 1210–1260 cm^{-1}. Bands characteristic of C–O stretching of the carbonate group emerged at 1210 and 1260 cm^{-1} along with 798 cm^{-1} characteristic out-of-plane bending of O– CO–O and 1599 cm^{-1} (C–C stretching) of benzene ring. The three bands presented in the range 2969 and 2860 (asymmetric and symmetric C–H stretching) remain [44, 45].

This structural analysis corroborates the expected results according to previously published articles for this type of material [46–48].

The polyurethane foam with bagasse ash (PFA) spectrum overlapped with the spectrum of polyurethane foam without ash (PF) (Fig. 1b). Both formulations exhibited similar bands and intensities without additional bands that belong to other chemical species, suggesting that sugarcane bagasse ash was not chemically bound to the polymer and consequently not incorporated in the molecular structure. Several results were reported for polyurethane made with fly ash, where only slight changes were observed in the composite foam spectrum with additional bands at about 680, 610, 595 and 460 cm^{-1} from the presence of aluminosilicate and silica [19].

Foams characterization

Both foams were easy to cut by a simple saw, releasing small and heavy particles. A visual inspection (Fig. 2) showed that the reinforced foam (PFA) presented smaller inner cells more homogenously distributed than the neat formulation (PF). The observation was confirmed by SEM analysis of the foams morphology (Fig. 3) since PF exhibited an average cell's size value of 496 nm and PAF a value of 480 nm. In the figure, the SEM micrographs the first visible feature was the irregular structure revealed by both (PF and PFA) conditions, with the latter presenting apparent damage of cells probably caused by ash presence [49, 50]. In addition to surface heterogeneity, PFA samples displayed micro-holes, in this case, due to the introduction of solid particles into the polyol premix that might significantly alter bubble nucleation conditions, which directly affects the size, shape, and number of pores, as well as pore wall thickness in the final materials [51]. The finer cell structure, associated to a reduction in foam density after the incorporation of particles showed a strong relationship with the increase of nucleating points in the reaction media facilitating, among other things, the process of bubbles formation [52–54].

Both bio-based foams exhibited high apparent densities (Table 4) with average values of 134.7 $kg.m^{-3}$ and (PF) and 105.7 $kg.m^{-3}$ (PFA). According to some authors, the filler particles act as nucleation sites that promote an increase in the number of cells formed with increasing filler content therefore promoting a reduction on foam density [20, 46, 55].

Table 4
PUR foams (PF and PFA), density, compressive strength, and specific compressive strength.

Sample	Density ($kg.m^{-3}$)	Compressive Strength (at 10%) (kPa)	Specific compressive strength ($m^2.s^{-2}$)
PF	134.7 ± 3.6	135.9 ± 3.0	1009
PFA	105.7 ± 10.1	121.5 ± 2.3	1149

Looking into the comparative stress-strain plot (Fig. 4), both foams showed the usual linear elastic region, yet PF behavior surpassed the typical plateau phase, progressing immediately to a steep increase in

stress indicative of the densification of the collapsed cell's walls [56]. PFA displayed a milder progression with a suggestion of plateau phase at higher strain rates [57].

The compressive strength values (Table 4) at 10% strain were 135.9 kPa (PF) and 121.5 kPa (PFA). The incorporation of 4.5% SCBA (grain size below 250 µm) was ineffective in the increment of the compressive strength, however, that small amount was enough to increase the foam's specific compressive strength from 1009 to 1149 $m^2.s^{-2}$. These results are weak within this density range when compared with foams made with sustainable Mannich polyols with cellulose, diatomite and walnut shell fillers [47]. The addition of 5% of fly ash (diameter below 25 µm) used as filler in fossil-based foams has increased in 14% the apparent density along with the compressive strength [19], suggesting that other factors (e.g. polyol feedstock, grain size, ash packing, etc.) are yet to be accounted.

It was observed in previous experiments, that the addition of higher percentages of ash resulted in an exponential increase in the polyol premix viscosity, inducing filler agglomeration, hindering foam rising, resulting in foams with very fragile structures, effects also observed in similar studies [20, 49]. The incorporation of 4.5% of ashes in the polyurethane foam was considered a hard limit and the synthesis was optimized accordingly.

Furthermore, ester-based polyols are usually more viscous and FDR-based polyol is an example (about 13256 mPa.s at room temperature) a factor that strongly affected polyurethane processability in laboratory conditions [58]. Recalling the FDR lipidic composition [25] and the derived polyol characterization (Table 3), that high viscosity is most probably due to the presence of epoxide oligomers that form hydrogen bonds in the presence of the hydroxyl groups generated in the ring-opening reaction [59] and the presence of waxes with crystallization temperature above room temperature [58].

On top of that, cross-linking vegetable-oil derived polyols with MDI can be compromised by steric hindrance introduced by the presence of secondary hydroxyl groups and long dangling hydrocarbon chains, affecting negatively the polymer network resistance to stress under load [60–62]. To improve the incorporation of this viscous polyol in the foam premix it was necessary to use heat, and the release of carbon dioxide (CO_2) gas bubbles as a product of reaction with the diisocyanate was trapped when the highly viscous mixture has cooled, restraining the expansion of cell's, hence conditioning cell's size and distribution, and therefore foam density and compressive strength [20, 59, 63, 64].

Observing the comparative thermogram obtained by DSC in Fig. 5, both PF and PFA exhibited overlapped intervals of decomposition onset temperatures related to the bio-polyol backbone in both materials, suggesting that sugarcane bagasse ash wasn't integrated in the polyurethane molecular structure [65].

In Table 5 are identified the different thermal events, glass transition temperature (T_g) and the decomposition onset temperatures (T_d), which is indicative of initial thermal degradation. T_g values of 74.0 and 71.8°C were found for both PF and PFA polyurethanes respectively, with a slight decrease associated with the incorporation of ash content. Those T_g values are close to the values previously

reported by similar studies [66, 67]. The decomposition onset temperatures were observed as narrow endothermic peaks in both samples above 200°C, indicating the beginning of thermal degradation, at 215.0 and 230.0°C for PA and PFA conditions respectively. For the reinforced foam an endothermic peak was observed at a higher temperature (247.0°C) which may be related to the presence of silica (2.7% wt.) in the ash.

Table 5
PUR foams (PF and PFA), thermal properties (T_g, T_m and k).

Sample	T_g (°C)	T_d (°C)	k ($W.m^{-1}.K^{-1}$)
PF	74.0	215.0–238.0	4.8×10^{-2}
PFA	71.8	230.0–247.0	4.6×10^{-2}
*Values from technical data sheet			

Thermal conductivity is mainly the result of a balance between the blowing gas content (e.g. CO_2 or other), foam density and cell's size [68, 69]. The thermal conductivity values (Table 5) were 0.048 $W.m^{-1}.K^{-1}$ (PF), and 0.046 $W.m^{-1}.K^{-1}$ (PFA), confirming that even with this limited amount, ash can reduce thermal conductivity. Similar results were described in a study conducted with tung oil-based polyol and rice husk ash up to 5% [20]. These values are also within the range of inorganic compounds like ceramics, cellular calcium silicate or glass as well natural fibers such as rice straw, wood and coconut fibers or cork without the inherent sensitivity to moisture [70].

To results of the flammability test ensued to limit their use for thermal insulation are compiled in Table 6 and the specimens after the ignitability test under open flame are represented in Fig. 6. The neat foam (PF) exhibited a higher burning length (132.3 mm) and burning time (251.7 s) and time of extinguishment (255.0 s) than the filled foam (56.7 mm, 90.3 s and 116.7 s, respectively). The remaining amount of sample after burning was about 57.4% for PF and 87.4% for PFA, respectively, despite the higher burning rate of PFA (38 $mm.min^{-1}$) compared with PF (33 $mm.\ min^{-1}$). Materials with rating HB by UL 94 standard for safety shall not have a burning rate exceeding 40 mm per minute over a 75 mm span for specimens having a thickness of 3.0 to 13 mm or cease to burn before the 100 mm reference mark. Both criteria were accomplished by the ash-filled foam.

Table 6
PUR foams (PF and PFA) flammability evaluation. Horizontal burning test results.

Samples	Burning time after flame (s)	Burning Length (mm)	Time Extinguishment (s)	PMR (%)	Burning rate ($mm.min^{-1}$)
PF	251.7 ± 41.7	132.3 ± 2.1	255.0 ± 49.5	57.4 ± 6.3	33 ± 6
PFA	90.3 ± 24.5	56.7 ± 17.0	116.7 ± 17.0	87.4 ± 7.8	38 ± 6

T extinguishment– time between application of burner flame and specimen flame extinguishment, s. Afterglow shall not be included in this time. PMR– percentual mass retained by the entire specimen. $PMR=(S_2/S_1) \times 100$, where S_2 is the mass of specimen after ignition (g) and S_1 before ignition (g).

It has been reported that ash from wastes rich in Si and Ca elements which are assigned for SiO_2 and $CaCO_3$, respectively, had a positive effect on flame retardancy of PU foams [22, 71, 72]. These results were in accordance with this work since silica (SiO_2) was the predominant mineral in the added ash accounting for 59.5% wt. (Table 2) and the addition of 4.5% SCBA to the foam formulation, amount to a total of 2.7% wt. in SiO_2 .The compound Fe_2O_3 was the second most abundant (17% wt.) in SCBA, and it was also tested for its flame-retardant potential in previous works. Hollow glass microspheres coated with Fe_2O_3 enhanced the flame retardant and smoke suppression in thermoplastic polyurethane [73]. In another work, when Fe_2O_3 particles were used in a mixture with PET at 1.2%, the limiting oxygen index increased by around 6%, the total heat release and smoke production decreased by 32% and 57%, respectively [74].

4. Conclusions

In this work, a bio-based water-blown polyurethane foam with fire-retardant properties was produced through the valorization of two by-products derived from Amyris industrial fermentation process, the microbial crude oil recovered after distillation, and the ash obtained after sugarcane bagasse burning for energy generation.

Microscopic observations showed a well-formed finer structure, albeit heterogeneous, paired with a lower foam density of the filled foam, suggesting that ash particles acted as nucleation sites during the foaming process promoting structural stabilization.

Polyurethane formulation was particularly challenging since the backbone is a polyol derived from a biowaste with a biphasic composition, prone to epoxide oligomerization and wax crystallization.

Within the high density range, both foams showed a relatively low mechanical performance suggesting that controlling polyol viscosity, hence foam porosity, particle size, and distribution in the matrix are crucial points. An adequate pretreatment of the microbial oil and implementing changes in the reaction system should impart improved results.

The absence of chemical interaction between ash filler and the polyurethane matrix and foam structure suggests that ash as a filler has a plasticizing effect increasing the polymer chain mobility, thus decreasing the glass transition temperature of the foam, delaying the decomposition onset temperature, and thermal conductivity. The thermal conductivity for both bio-based foams was in the range of inorganic compounds such as ceramics, cellular calcium silicate, or cellular glass, along with natural fibers (e.g. coconut and cork), without the inherent sensitivity to moisture.

The flammability test results suggest that sugarcane bagasse ash has improved the foam performance in compliance with the fire protection standard UL 94, class HB.

Notwithstanding the need to further improvement, the results corroborate the idea that polyurethane foams derived from suitable and renewable waste by-products constitute a sustainable green alternative to both edible and fossil-based sources and that sugarcane bagasse ash can be an acceptable source of silica for the reinforcement of new sustainable composites with reduced flammability eventually replacing harmful chemicals used with the same purpose.

Declarations

Acknowledgments: Work funded by AICEP (Agência para o Investimento e Comércio Externo de Portugal, E. P. E) through Alchemy – Capturing High Value from Industrial Fermentation Bio Products. Granting agency: Portugal 2020, European Regional Development Fund (FEDER).

Base Funding - UIDB/04708/2020 and Programmatic Funding - UIDP/04708/2020 of the CONSTRUCT - Instituto de I&D em Estruturas e Construções - funded by national funds through the FCT/MCTES (PIDDAC).

Conflicts of Interest: The authors declare no conflict of interest.

References

1. Morseletto, P.: Targets for a circular economy. Resour. Conserv. Recycl. 153, 104553 (2020). https://doi.org/https://doi.org/10.1016/j.resconrec.2019.104553
2. Höök, M., Davidsson, S., Johansson, S., Tang, X.: Decline and depletion rates of oil production: a comprehensive investigation. Philos. Trans. R. Soc. A Math. Phys. Eng. Sci. 372, 20120448 (2014). https://doi.org/10.1098/rsta.2012.0448
3. Sorrell, S., Speirs, J., Bentley, R., Brandt, A., Miller, R.: Global oil depletion: A review of the evidence. Energy Policy. 38, 5290–5295 (2010). https://doi.org/10.1016/j.enpol.2010.04.046

4. Di Bartolo, A., Infurna, G., Dintcheva, N.T.: A review of bioplastics and their adoption in the circular economy. Polymers (Basel). 13, (2021). https://doi.org/10.3390/polym13081229
5. Waghmare, B., Mahanwar, P., Waghmare, B., Mahanwar, P.: Review on synthesis of isocyanate free polyurethane using sustainable routes and its applications Reprinted from PAINTINDIA May 2019 Review on synthesis of isocyanate free polyurethane using sustainable routes and its applications. (2019)
6. Das, A., Mahanwar, P.: A brief discussion on advances in polyurethane applications. Adv. Ind. Eng. Polym. Res. 3, 93–101 (2020). https://doi.org/10.1016/j.aiepr.2020.07.002
7. Shoaib, S., Shahzad Maqsood, K., Nafisa, G., Waqas, A., Muhammad, S., Tahir, J.: A Comprehensive Short Review on Polyurethane Foam. Int. J. Innov. Appl. Stud. 12, 165–169 (2014)
8. Berardi, U.: The impact of aging and environmental conditions on the effective thermal conductivity of several foam materials. Energy. 182, 777–794 (2019). https://doi.org/10.1016/j.energy.2019.06.022
9. Wittbecker, W., Daems; D., Werther, U.: Performance of polyurethane (PUR) building products in fires, https://www.isopa.org/media/1136, (2011)
10. Tenorio-Alfonso, A., Sánchez, M.C., Franco, J.M.: A Review of the Sustainable Approaches in the Production of Bio-based Polyurethanes and Their Applications in the Adhesive Field. J. Polym. Environ. 28, 749–774 (2020). https://doi.org/10.1007/s10924-020-01659-1
11. Kaikade, D.S., Sabnis, A.S.: Polyurethane foams from vegetable oil-based polyols: a review. Polym. Bull. 80, 2239–2261 (2023). https://doi.org/10.1007/s00289-022-04155-9
12. Patil, C.K., Jung, D.W., Jirimali, H.D., Baik, J.H., Gite, V. V., Hong, S.C.: Nonedible Vegetable Oil-Based Polyols in Anticorrosive and Antimicrobial Polyurethane Coatings. Polymers (Basel). 13, 3149 (2021). https://doi.org/10.3390/polym13183149
13. Dang, Y., Luo, X., Wang, F., Li, Y.: Value-added conversion of waste cooking oil and post-consumer PET bottles into biodiesel and polyurethane foams. Waste Manag. 52, 360–366 (2016). https://doi.org/10.1016/j.wasman.2016.03.054
14. Athawale, V.D., Nimbalkar, R. V.: Polyurethane dispersions based on sardine fish oil, soybean oil, and their interesterification products. J. Dispers. Sci. Technol. 32, 1014–1022 (2011). https://doi.org/10.1080/01932691.2010.497459
15. Uprety, B.K., Reddy, J.V., Dalli, S.S., Rakshit, S.K.: Utilization of microbial oil obtained from crude glycerol for the production of polyol and its subsequent conversion to polyurethane foams. Bioresour. Technol. 235, 309–315 (2017). https://doi.org/10.1016/j.biortech.2017.03.126
16. Samavi, M., Rakshit, S.: Utilization of Microbial Oil from Poplar Wood Hemicellulose Prehydrolysate for the Production of Polyol Using Chemo-enzymatic Epoxidation. 335, 327–335 (2020). https://doi.org/10.1007/s12257-019-0416-8
17. Ramanujam, S., Zequine, C., Bhoyate, S., Neria, B., Kahol, P., Gupta, R.: Novel Biobased Polyol Using Corn Oil for Highly Flame-Retardant Polyurethane Foams. C. 5, 13 (2019). https://doi.org/10.3390/c5010013

18. Mngomezulu, M.E., John, M.J., Jacobs, V., Luyt, A.S.: Review on flammability of biofibres and biocomposites. Carbohydr. Polym. 111, 149–182 (2014). https://doi.org/https://doi.org/10.1016/j.carbpol.2014.03.071
19. Kuźnia, M., Magiera, A., Pielichowska, K., Ziąbka, M., Benko, A., Szatkowski, P., Jerzak, W.: Fluidized bed combustion fly ash as filler in composite polyurethane materials. Waste Manag. 92, 115–123 (2019). https://doi.org/https://doi.org/10.1016/j.wasman.2019.05.012
20. Ribeiro Da Silva, V., Mosiewicki, M.A., Yoshida, M.I., Coelho Da Silva, M., Stefani, P.M., Marcovich, N.E.: Polyurethane foams based on modified tung oil and reinforced with rice husk ash I: Synthesis and physical chemical characterization. Polym. Test. 32, 438–445 (2013). https://doi.org/10.1016/j.polymertesting.2013.01.002
21. Ali, M.H.M., Rahman, H.A., Amirnordin, S.H., Khan, N.A.: Eco-Friendly Flame-Retardant Additives for Polyurethane Foams: A Short Review. Key Eng. Mater. 791, 19–28 (2018). https://doi.org/10.4028/www.scientific.net/KEM.791.19
22. Kairytė, A., Kremensas, A., Vaitkus, S., Członka, S., Strąkowska, A.: Fire Suppression and Thermal Behavior of Biobased Rigid Polyurethane Foam Filled with Biomass Incineration Waste Ash. Polymers (Basel). 12, 683 (2020). https://doi.org/10.3390/polym12030683
23. Licht, S.: Chapter 5 - Fermentation for Biofuels and Bio-Based Chemicals. In: Henry C. Vogel, C.M.T. (ed.) Fermentation and Biochemical Engineering Handbook. pp. 59–82. Elsevier (2014)
24. Benjamin, K.R., Silva, I.R., Cherubim, J.P., McPhee, D., Paddon, C.J.: Developing commercial production of semi-synthetic artemisinin, and of β-Farnesene, an Isoprenoid Produced by Fermentation of Brazilian Sugar. J. Braz. Chem. Soc. 27, 1339–1345 (2016). https://doi.org/10.5935/0103-5053.20160119
25. Teixeira, F.S., Vidigal, S.S.M.P., Pimentel, L.L., Costa, P.T., Tavares-Valente, D., Azevedo-Silva, J., Pintado, M.E., Fernandes, J.C., Rodríguez-Alcalá, L.M.: Phytosterols and Novel Triterpenes Recovered from Industrial Fermentation Coproducts Exert In Vitro Anti-Inflammatory Activity in Macrophages. Pharmaceuticals. 14, 583 (2021). https://doi.org/10.3390/ph14060583
26. Li, Y.Y., Luo, X., Hu, S.: Bio-based Polyols and Polyurethanes. Bio-based Polyols and Polyurethanes. 1–79 (2015). https://doi.org/10.1007/978-3-319-21539-6
27. Hattimattur, V., Sangale, V.R., Zade, P.S., Mandake, M.B., Walke, S., Mumbai, N.: Review: Epoxidation of Vegetable oils. Int. J. Trend Res. Dev. 5, 542–548 (2018)
28. Abril-Milán, D., Valdés, O., Mirabal-Gallardo, Y., de la Torre, A.F., Bustamante, C., Contreras, J.: Preparation of renewable bio-polyols from two species of Colliguaja for Rigid polyurethane foams. Materials (Basel). 11, 1–20 (2018). https://doi.org/10.3390/ma11112244
29. Guo, Y., Hardesty, J.H., Mannari, V.M., Massingill, J.L.: Hydrolysis of epoxidized soybean oil in the presence of phosphoric acid. JAOCS, J. Am. Oil Chem. Soc. 84, 929–935 (2007). https://doi.org/10.1007/s11746-007-1126-5
30. Pfister, D.P., Xia, Y., Larock, R.C.: Recent Advances in Vegetable Oil-Based Polyurethanes. ChemSusChem. 4, 703–717 (2011). https://doi.org/10.1002/cssc.201000378

31. Niyogi, D., Kumar, R., Gandhi, K.S.: Water blown free rise polyurethane foams. Polym. Eng. Sci. 39, 199–209 (1999). https://doi.org/10.1002/pen.11408
32. Ionescu, M.: Chemistry and Technology of Polyols for Polyurethane Volume 2. (2016)
33. Barrera Torres, G., Dognani, G., da Silva Agostini, D.L., dos Santos, R.J., Camargo Cabrera, F., Gutierrez Aguilar, C.M., de Paiva, F.F.G., Rainho Teixeira, S., Job, A.E.: Potential Eco-friendly Application of Sugarcane Bagasse Ash in the Rubber Industry. Waste and Biomass Valorization. 12, 4599–4613 (2021). https://doi.org/10.1007/s12649-020-01309-6
34. Zieleniewska, M., Leszczyński, M.K., Kurańska, M., Prociak, A., Szczepkowski, L., Krzyżowska, M., Ryszkowska, J.: Preparation and characterisation of rigid polyurethane foams using a rapeseed oil-based polyol. Ind. Crops Prod. 74, 887–897 (2015). https://doi.org/https://doi.org/10.1016/j.indcrop.2015.05.081
35. Lu, Y., Larock, R.C.: Soybean-Oil-Based Waterborne Polyurethane Dispersions: Effects of Polyol Functionality and Hard Segment Content on Properties. Biomacromolecules. 9, 3332–3340 (2008). https://doi.org/10.1021/bm801030g
36. Coman, A.E., Peyrton, J., Hubca, G., Sarbu, A., Gabor, A.R., Nicolae, C.A., Iordache, T.V., Averous, L.: Synthesis and characterization of renewable polyurethane foams using different biobased polyols from olive oil. Eur. Polym. J. 149, 110363 (2021). https://doi.org/10.1016/j.eurpolymj.2021.110363
37. Cifarelli, A., Boggioni, L., Vignali, A., Tritto, I., Bertini, F., Losio, S.: Flexible Polyurethane Foams from Epoxidized Vegetable Oils and a Bio-Based Diisocyanate. Polymers (Basel). 13, 612 (2021). https://doi.org/10.3390/polym13040612
38. Ang, K.P., Lee, C.S., Cheng, S.F., Chuah, C.H.: Synthesis of palm oil-based polyester polyol for polyurethane adhesive production. J. Appl. Polym. Sci. 131, n/a-n/a (2014). https://doi.org/10.1002/app.39967
39. Ghasemlou, M., Daver, F., Ivanova, E.P., Adhikari, B.: Polyurethanes from seed oil-based polyols: A review of synthesis, mechanical and thermal properties. Ind. Crops Prod. 142, 111841 (2019). https://doi.org/https://doi.org/10.1016/j.indcrop.2019.111841
40. Echeverria-Altuna, O., Ollo, O., Larraza, I., Gabilondo, N., Harismendy, I., Eceiza, A.: Effect of the biobased polyols chemical structure on high performance thermoset polyurethane properties. Polymer (Guildf). 263, 125515 (2022). https://doi.org/10.1016/j.polymer.2022.125515
41. Dhaliwal, G.S., Anandan, S., Chandrashekhara, K., Lees, J., Nam, P.: Development and characterization of polyurethane foams with substitution of polyether polyol with soy-based polyol. Eur. Polym. J. 107, 105–117 (2018). https://doi.org/10.1016/j.eurpolymj.2018.08.001
42. Mihoubi, W., Sahli, E., Gargouri, A., Amiel, C.: FTIR spectroscopy of whole cells for the monitoring of yeast apoptosis mediated by p53 over-expression and its suppression by Nigella sativa extracts. PLoS One. 12, (2017). https://doi.org/10.1371/journal.pone.0180680
43. Shapaval, V., Afseth, N.K., Vogt, G., Kohler, A.: Fourier transform infrared spectroscopy for the prediction of fatty acid profiles in Mucor fungi grown in media with different carbon sources. Microb. Cell Fact. 13, 1–11 (2014). https://doi.org/10.1186/1475-2859-13-86

44. Jiang, L., Ren, Z., Zhao, W., Liu, W., Liu, H., Zhu, C.: Synthesis and structure/properties characterizations of four polyurethane model hard segments. R. Soc. Open Sci. 5, (2018). https://doi.org/10.1098/rsos.180536
45. Rogulska, M., Kultys, A., Pikus, S.: The effect of chain extender structure on the properties of new thermoplastic poly(carbonate–urethane)s derived from MDI. J. Therm. Anal. Calorim. 127, 2325–2339 (2017). https://doi.org/10.1007/s10973-016-5756-4
46. Hejna, A., Kopczyńska, M., Kozłowska, U., Klein, M., Kosmela, P., Piszczyk, Ł.: Foamed Polyurethane Composites with Different Types of Ash – Morphological, Mechanical and Thermal Behavior Assessments. Cell. Polym. 35, 287–308 (2016). https://doi.org/10.1177/026248931603500601
47. De Luca Bossa, F., Santillo, C., Verdolotti, L., Campaner, P., Minigher, A., Boggioni, L., Losio, S., Coccia, F., Iannace, S., Lama, G.C.: Greener Nanocomposite Polyurethane Foam Based on Sustainable Polyol and Natural Fillers: Investigation of Chemico-Physical and Mechanical Properties. Materials (Basel). 13, 211 (2020). https://doi.org/10.3390/ma13010211
48. Ku, M., Magiera, A., Zygmunt-kowalska, B., Kaczorek-chrobak, K.: Fly Ash as an Eco-Friendly Filler for Rigid Polyurethane Foams Modification. (2021)
49. Uram, K., Kurańska, M., Andrzejewski, J., Prociak, A.: Rigid polyurethane foams modified with biochar. Materials (Basel). 14, 1–14 (2021). https://doi.org/10.3390/ma14195616
50. Kuźnia, M., Zygmunt-Kowalska, B., Szajding, A., Magiera, A., Stanik, R., Gude, M.: Comparative Study on Selected Properties of Modified Polyurethane Foam with Fly Ash. Int. J. Mol. Sci. 23, (2022). https://doi.org/10.3390/ijms23179725
51. Leszczyńska, M., Malewska, E., Ryszkowska, J., Kurańska, M., Gloc, M., Leszczyński, M.K., Prociak, A.: Vegetable Fillers and Rapeseed Oil-Based Polyol as Natural Raw Materials for the Production of Rigid Polyurethane Foams. Materials (Basel). 14, 1772 (2021). https://doi.org/10.3390/ma14071772
52. Merillas, B., Villafañe, F., Rodríguez-Pérez, M.Á.: Nanoparticles Addition in PU Foams: The Dramatic Effect of Trapped-Air on Nucleation. Polymers (Basel). 13, 2952 (2021). https://doi.org/10.3390/polym13172952
53. Lorusso, C., Vergaro, V., Monteduro, A., Saracino, A., Ciccarella, G., Congedo, P.M., Scremin, B.F.: Characterization of Polyurethane Foam Added with Synthesized Acetic and Oleic-Modified TiO 2 Nanocrystals. Nanomater. Nanotechnol. 5, 26 (2015). https://doi.org/10.5772/61275
54. Chen, Y., Das, R., Battley, M.: Effects of cell size and cell wall thickness variations on the strength of closed-cell foams. Int. J. Eng. Sci. 120, 220–240 (2017). https://doi.org/10.1016/j.ijengsci.2017.08.006
55. Akkoyun, M., Akkoyun, S.: Blast furnace slag or fly ash filled rigid polyurethane composite foams: A comprehensive investigation. J. Appl. Polym. Sci. 47433 (2019). https://doi.org/10.1002/app.47433
56. Mane, J.V., Chandra, S., Sharma, S., Ali, H., Chavan, V.M., Manjunath, B.S., Patel, R.J.: Mechanical Property Evaluation of Polyurethane Foam under Quasi-static and Dynamic Strain Rates- An Experimental Study. Procedia Eng. 173, 726–731 (2017). https://doi.org/10.1016/j.proeng.2016.12.160

57. Tu, Z.H., Shim, V.P.W., Lim, C.T.: Plastic deformation modes in rigid polyurethane foam under static loading. Int. J. Solids Struct. 38, 9267–9279 (2001). https://doi.org/10.1016/S0020-7683(01)00213-X
58. Marcovich, N.E., Kurańska, M., Prociak, A., Malewska, E., Bujok, S.: The effect of different palm oil-based bio-polyols on foaming process and selected properties of porous polyurethanes. Polym. Int. 66, 1522–1529 (2017). https://doi.org/10.1002/pi.5408
59. Ji, D., Fang, Z., He, W., Luo, Z., Jiang, X., Wang, T., Guo, K.: Polyurethane rigid foams formed from different soy-based polyols by the ring opening of epoxidised soybean oil with methanol, phenol, and cyclohexanol. Ind. Crops Prod. 74, 76–82 (2015). https://doi.org/10.1016/j.indcrop.2015.04.041
60. Narine, S.S., Kong, X., Bouzidi, L., Sporns, P.: Physical properties of polyurethanes produced from polyols from seed oils: II. Foams. JAOCS, J. Am. Oil Chem. Soc. 84, 65–72 (2007). https://doi.org/10.1007/s11746-006-1008-2
61. Pillai, P.K.S., Li, S., Bouzidi, L., Narine, S.S.: Metathesized palm oil polyol for the preparation of improved bio-based rigid and flexible polyurethane foams. Ind. Crops Prod. 83, 568–576 (2016). https://doi.org/10.1016/j.indcrop.2015.12.068
62. Prociak, A., Kurańska, M., Uram, K., Wójtowicz, M.: Bio-Polyurethane Foams Modified with a Mixture of Bio-Polyols of Different Chemical Structures. Polymers (Basel). 13, 2469 (2021). https://doi.org/10.3390/polym13152469
63. Sundang, M., Nurdin, N.S., Saalah, S., Singam, Y.J., Al Edrus, S.S.A.O., Ismail, N.M., Sipaut, C.S., Abdullah, L.C.: Synthesis of Jatropha-Oil-Based Polyester Polyol as Sustainable Biobased Material for Waterborne Polyurethane Dispersion. Polymers (Basel). 14, (2022). https://doi.org/10.3390/polym14183715
64. Dzulkifli, M.H., Yahya, M.Y., Md Akhir, F.S., Majid, R.A.: Development of rigid biocomposite polyurethane foam for load bearing application. J. Teknol. (Sciences Eng. 68, 53–56 (2014). https://doi.org/10.11113/jt.v68.2929
65. Zhang, Q., Lin, X., Chen, W., Zhang, H., Han, D.: Modification of rigid polyurethane foams with the addition of nano-SiO2 or lignocellulosic biomass. Polymers (Basel). 12, (2020). https://doi.org/10.3390/polym12010106
66. Foams, P., Gu, R., Sain, M.M.: Effects of Wood Fiber and Microclay on the Performance of Soy Based Effects of Wood Fiber and Microclay on the Performance of Soy Based Polyurethane Foams. (2014). https://doi.org/10.1007/s10924-012-0538-y
67. Konar, S., Sain, M.: Preparation and Characterization of Sustainable Polyurethane Foams from Preparation and Characterization of Sustainable Polyurethane Foams from Soybean Oils. (2012). https://doi.org/10.1007/s11746-012-2109-8
68. Jarfelt, U., Ramnäs, O.: Thermal conductivity of polyurethane foam - best performance Thermal conductivity of polyurethane foam Best performance. 10th Int. Symp. Dist. Heat. Cool. 12 (2006)
69. Andersons, J., Kirpluks, M., Cabulis, P., Kalnins, K., Cabulis, U.: Bio-based rigid high-density polyurethane foams as a structural thermal break material, (2020)

70. Hung Anh, L.D., Pásztory, Z.: An overview of factors influencing thermal conductivity of building insulation materials. J. Build. Eng. 44, 102604 (2021). https://doi.org/10.1016/j.jobe.2021.102604
71. Kairytė, A., Kirpluks, M., Ivdre, A., Cabulis, U., Vaitkus, S., Pundienė, I.: Cleaner production of polyurethane foam: Replacement of conventional raw materials, assessment of fire resistance and environmental impact. J. Clean. Prod. 183, 760–771 (2018). https://doi.org/https://doi.org/10.1016/j.jclepro.2018.02.164
72. Liu, H., Zhang, B., Han, J.: Improving the Flame Retardancy and Smoke Suppression Properties of Polyurethane Foams with SiO2 Microcapsule and its Flame-Retardant Mechanism. Polym. Plast. Technol. Eng. 57, 1139–1149 (2018). https://doi.org/10.1080/03602559.2017.1373398
73. Jiao, C., Zhao, L., Chen, X.: Preparation of modified hollow glass microspheres using Fe2O3 and its flame retardant properties in thermoplastic polyurethane. J. Therm. Anal. Calorim. 127, 2101–2112 (2017). https://doi.org/10.1007/s10973-016-5831-x
74. Mei, N., Mingshuo, Z., Baoxia, X., Ruihong, Q., Mingqiang, S., Li, Z.: Introducing the Fe2O3 particles into fiber for flame retardancy and smoke suppression. J. Text. Inst. 1–7 (2022). https://doi.org/10.1080/00405000.2022.2026580

Figures

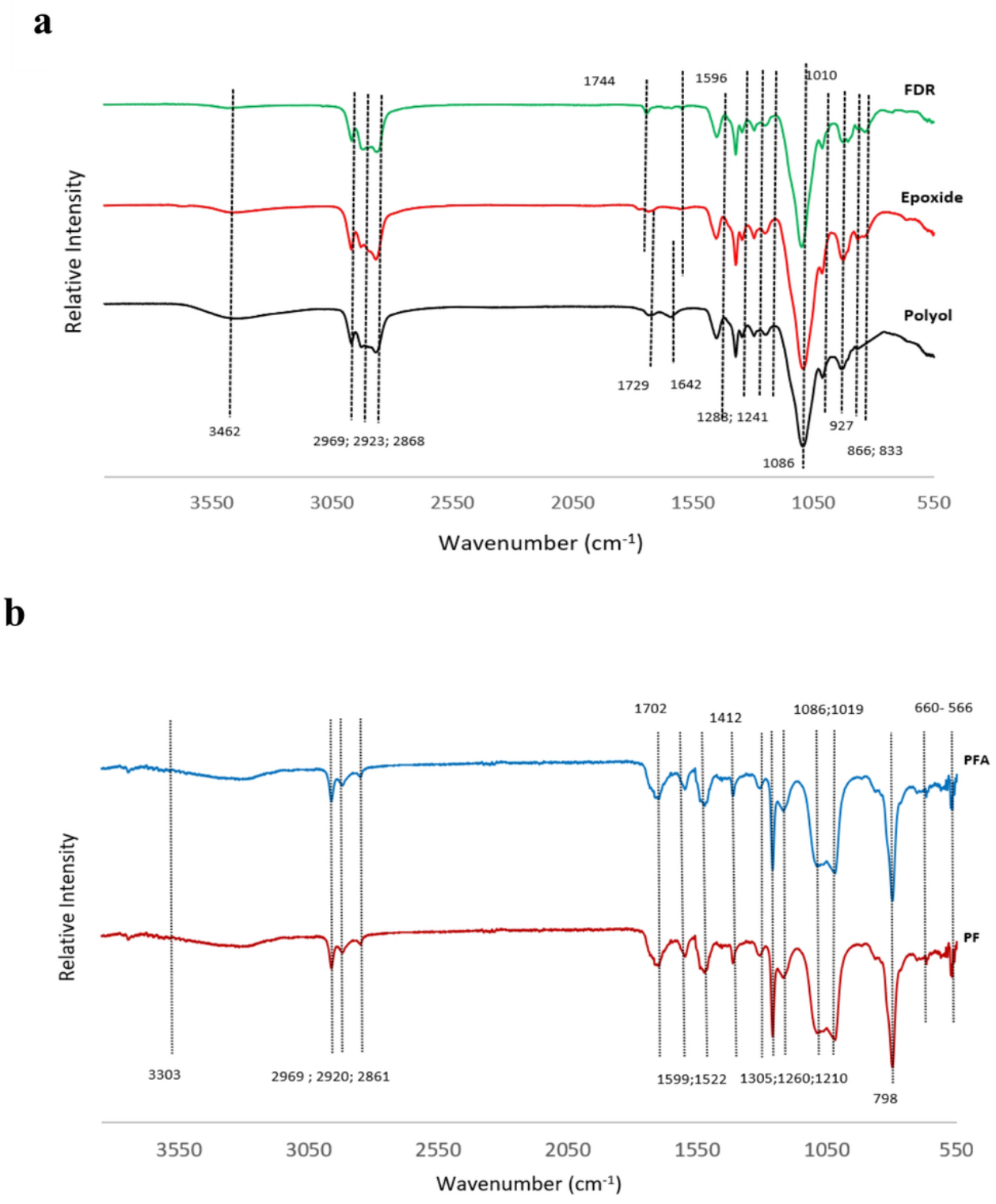

Figure 1

Structural analysis (FTIR), (a) reaction progression starting with the oily residue (FDR), the respective epoxide and subsequent polyol; (b) comparative structural analysis of both PUR foams (PF and PFA)

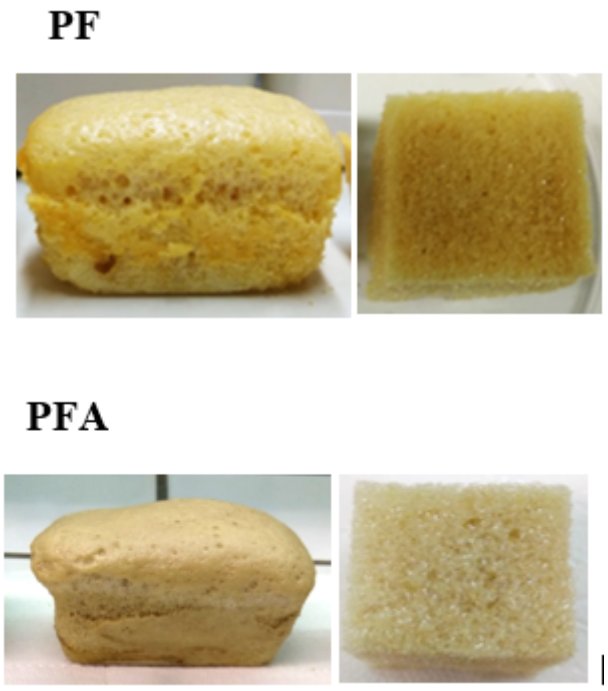

Figure 2

Representative bio-based PURfoams (PF and PFA)

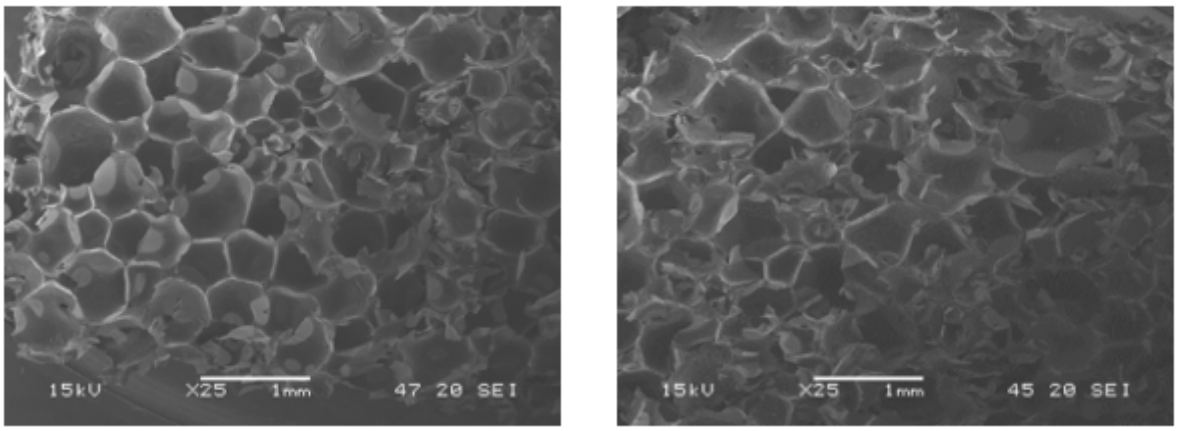

Figure 3

Representative SEM micrographs of both PUR bio-based foams (PF and PFA) , with pore size diameter average values

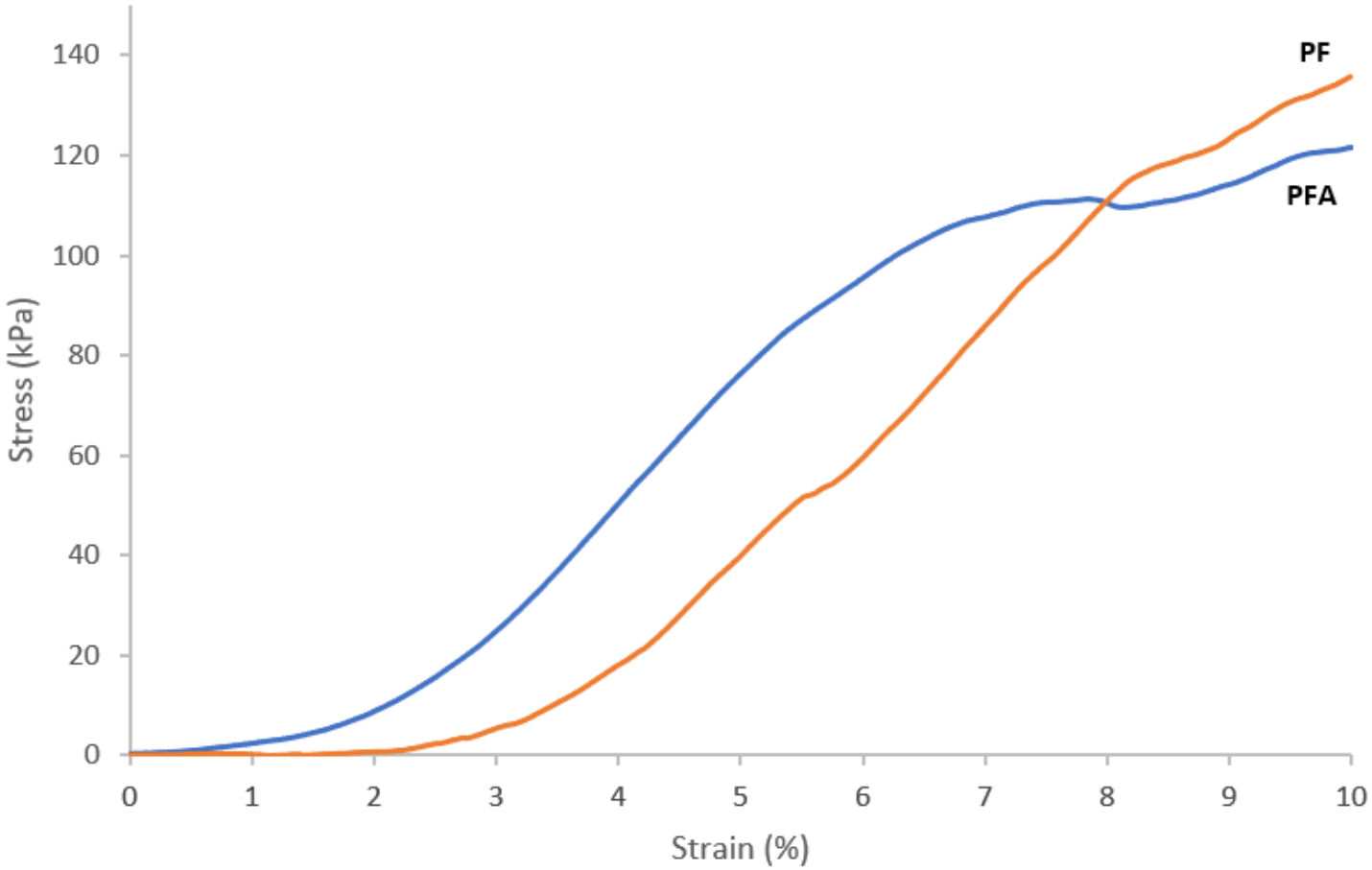

Figure 4

Strain-stress comparative plot of both PUR foams, (PF and PFA)

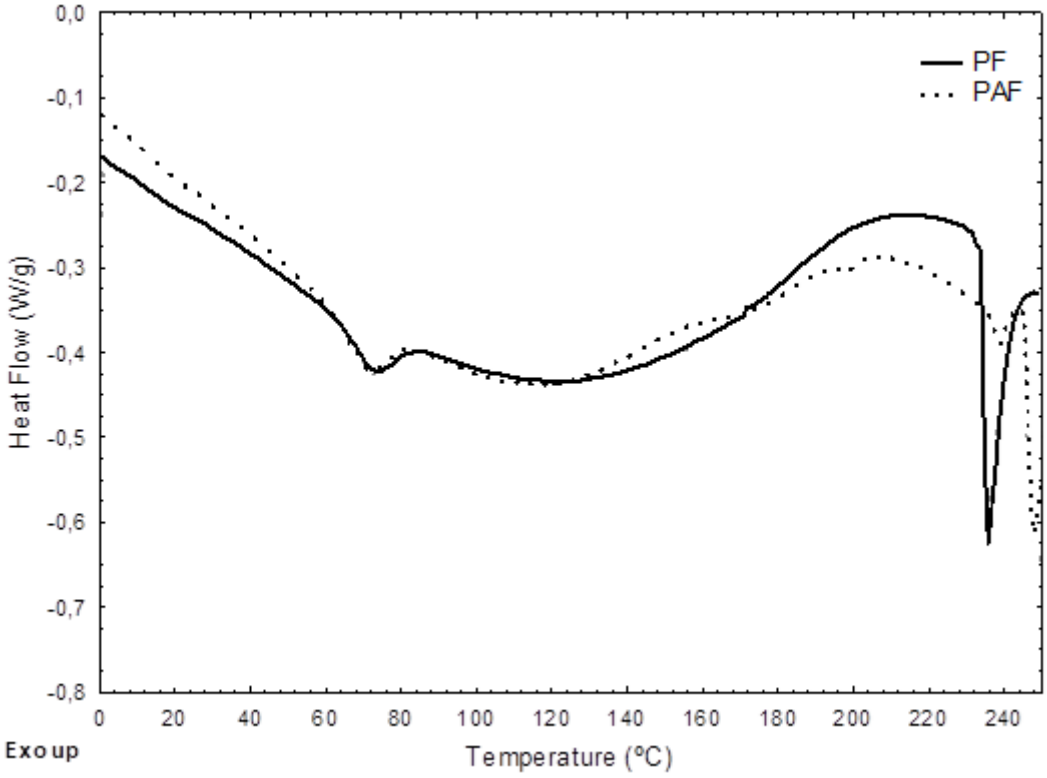

Figure 5

Comparative thermogram (DSC) of both PUR foams, (PF and PFA)

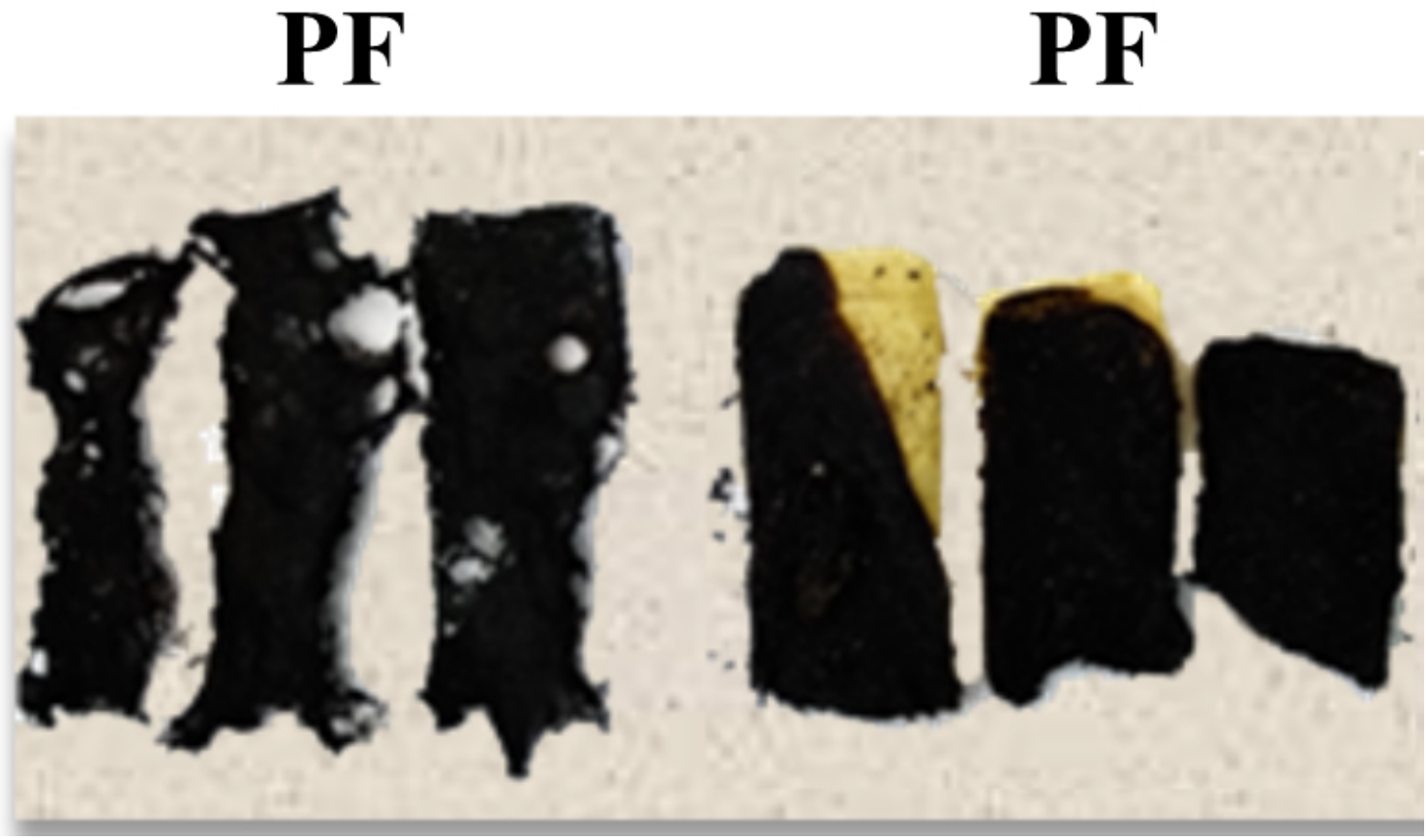

Figure 6

Pictures of both bio-based PUR foams, PF and PFA, after flammability tests